Investigation of the pseudoelastic behaviour in two commercial NiTi alloys: experiments and modelling

Casper van der Eijk[a], Jim Stian Olsen[b], and Zhiliang Z. L. Zhang[b]

[a] SINTEF Materials and Chemistry, Alfred Getz vei 2, 7465 Trondheim, Norway; casper.eijk@sintef.no
[b] Department of Structural Engineering, Norwegian University of Science and Technology, 7491 Trondheim, Norway; zhiliang.zhang@ntnu.no

Abstract. The purpose of the work is to test the suitability of commercially available NiTi alloys for application as seismic protection material. Two different NiTi alloys are characterized mechanically. One of these alloys is fully austenitic at room temperature, while the other has an austenite start temperature above room temperature, but a martensite start temperature below room temperature. The two alloys show only a small temperature region with pseudoelastic behaviour. Modelling was performed to investigate whether combining two different materials in one damper configuration provides a damper with a broad range of temperatures with good damping characteristics.

Key words: shape memory alloys, damping, pseudoelasticity.

1. INTRODUCTION

Although shape memory alloys (SMAs) have been known for decades, they have not been widely used in the civil structures. Due to their high damping capacity, there has been a recent interest in application of SMAs to seismic damping [1–5].

Shape memory alloys are mostly known for their ability to revert to their initial shape upon heating. This is called the shape memory effect. Another important phenomenon is the so-called pseudoelasticity or superelasticity in which the phase transformation from austenite to martensite occurs merely by increasing the external stress. The alloy undergoes the reverse transformation to the austenite state automatically by unloading the stress. The stress–strain curve for the pseudoelasticity shows a distinctive plateau and a hysteresis. This pseudo-

elastic behaviour exhibits good damping capacity because of the necessary energy for the phase transformations. The objective of the work is to characterize two commercially available NiTi alloys and investigate their suitability for application as seismic protection material.

2. EXPERIMENTAL

2.1. Materials

Two different NiTi alloys designated AF5 and AF30 were purchased from Grikin (China). The wires had a diameter of 2 mm. The chemical analyses of the two alloys are listed in Table 1. The transformation temperatures (A_s = austenite start, A_f = austenite finish, M_s = martensite start, and A_f = martensite finish) of materials are listed in Table 2. The transformation temperatures of the AF5 alloy are expected to be lower than the transformation temperatures of the AF30 alloy, since the presence of a higher Ni content generally decreases the transformation temperatures [6]. More details about the materials are available in [7].

2.2. Modelling

The mechanical behaviour of NiTi materials was modelled using Brinson's [8] model and programmed using MATLAB. Details of the modelling work are reported in Olsen [9]. The material parameters necessary for the Brinson model are calculated from stress–strain curves at various temperatures. These are as follows:

- elasticity modulus for the austenitic phase (D_A),
- elasticity modulus for the stress-induced martensite phase (D_M),
- critical stress for transformation start at $T < M_s$ ($\sigma_S^{M' \to M}$),
- critical stress for transformation ending at $T < M_s$ ($\sigma_f^{M' \to M}$),

Table 1. Chemical composition of the two NiTi alloys, %

	Ni	Ti	C
AF5	50.0	49.7	0.27
AF30	49.2	50.6	0.27

Table 2. Phase transformation temperatures of NiTi materials, °C. A_s = austenite start, A_f = austenite finish, M_s = martensite start, A_f = martensite finish

	A_s	A_f	M_s	M_f
AF5	−5	4	−40	−52
AF30	30	41	−53	−67

- slope of the critical transformation stress – temperature curves for forward transformation (C_M),
- slope of the critical transformation stress – temperature curves for reverse transformation (C_A),
- maximum residual strain (ε_L).

2.3. Mechanical characterization

Tensile tests were performed using a Dartec M1000RK servo hydraulic tensile testing machine connected to an Instron 8800 Digital Controller. A heat chamber with a temperature range between $-150\,°C$ and $250\,°C$ was used to control the specimen temperature. The displacement was registered using an extensometer. The temperature of the specimen surface was measured using a thermocouple. The length of the wire specimens was 200 mm.

3. RESULTS AND DISCUSSION

The AF5 material is a NiTi alloy with an A_f temperature of $4\,°C$ (see Table 2). The stress–strain curves for the AF5 material are shown in Fig. 1. The tested material exhibits a wide hysteresis and a small temperature range for pseudoelasticity. A more elaborate discussion and results of fatigue testing of this material are reported in [7]. Although the material has obviously its limitations when used as a seismic damping material, it is used to provide the parameters necessary for the modelling. At temperatures below the M_s the critical stress, $\sigma_S^{M'\to M}$, is nearly constant, as shown in Fig. 1a–c. From Fig. 1b it can be found that $\sigma_S^{M'\to M} = 72.7$ MPa and $\sigma_f^{M'\to M} = 296.9$ MPa.

The only stress–strain curve with distinct linear deformation of stress-induced martensite is found at $-20\,°C$, thus the elasticity modulus for stress-induced martensite, D_M, is obtained from Fig. 1d. From the same figure the maximum residual stress, ε_L, is obtained. At $T = 10\,°C$ the material is completely in the austenitic phase and the elasticity modulus for austenite, D_A, is measured from Fig. 1h. When $T > M_s$, the critical transformation stress, $\sigma_s^{A\to M}$, increases with temperature. A similar behaviour can be observed for $\sigma_s^{M\to A}$ when $T \geq A_s$. Figure 2 shows the critical stresses versus temperature. A linear regression was used to determine the parameters C_M and C_A. The respective values are 8.0 MPa/°C and 7.3 MPa/°C.

The AF30 material is a NiTi alloy with an austenite finish temperature, A_f, of $41\,°C$ (see Table 2). Figure 3 shows the stress–strain curves for this material. At temperatures $T \leq M_s$ the critical stress, $\sigma_s^{M'\to M}$, is nearly constant as shown in Fig. 3a–c. The values of the critical stresses, $\sigma_s^{M'\to M}$ and $\sigma_f^{M'\to M}$, can be obtained from these figures. The elasticity modulus for the stress-induced martensite, D_M, and maximum residual strain, ε_L, are obtained from the curve at $T = -53\,°C$ (Fig. 3c). The elasticity modulus for austenite, D_A, is measured
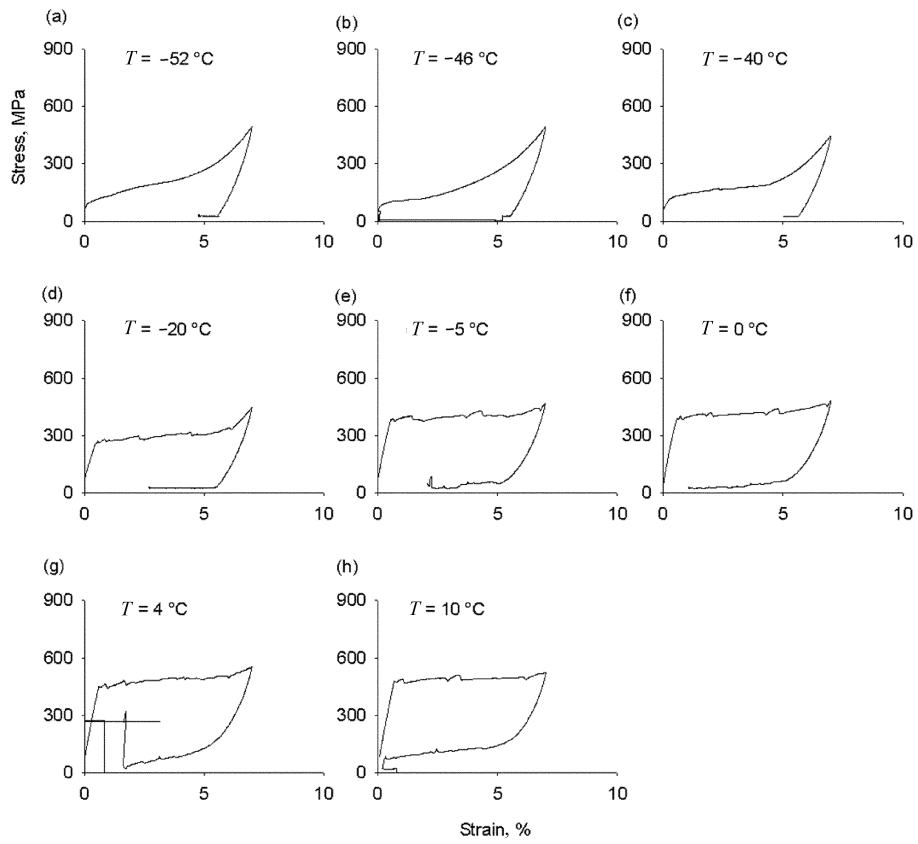
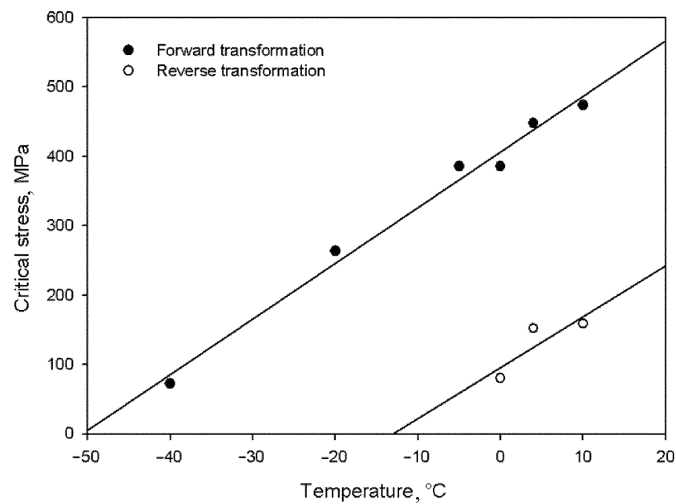**Fig. 1.** Tensile testing results of the AF5 material at various temperatures.

Fig. 2. Critical transformation stresses for forward and reverse transformation as a function of temperature for the AF5 material.
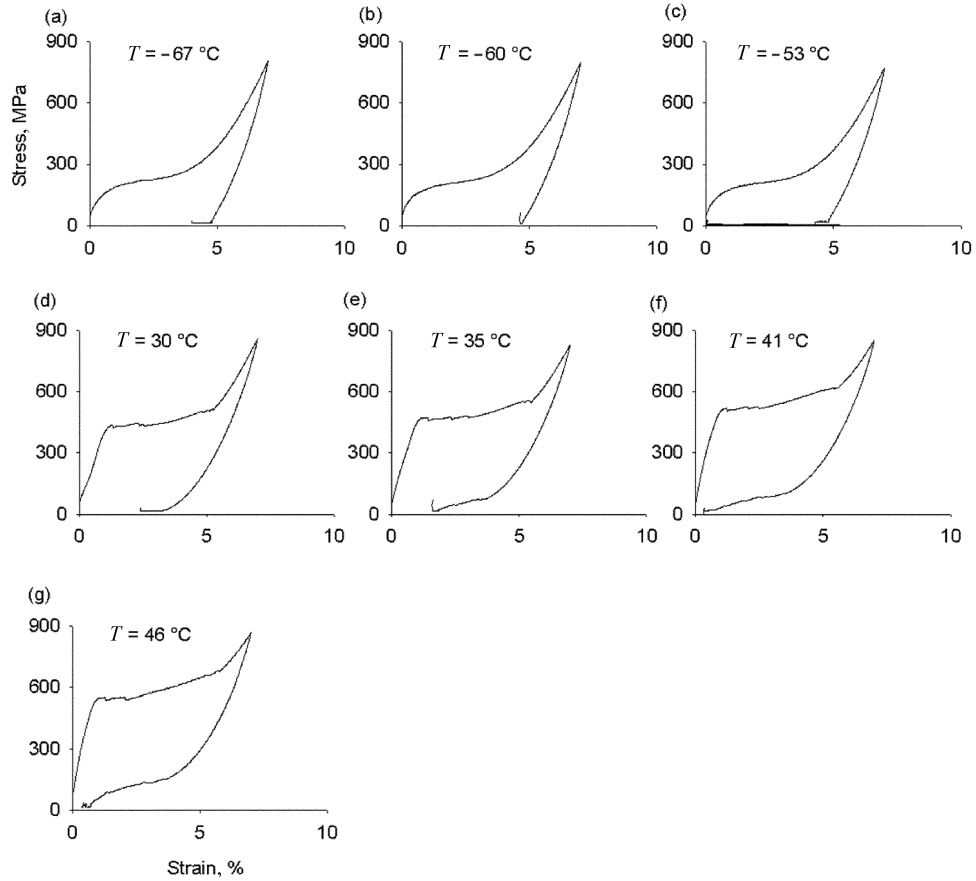
Fig. 3. Tensile testing results of the AF30 material at various temperatures.

at $T = 46\,°C$ (Fig. 3g), when the material is completely in the austenitic phase. Similar to the AF5 material, the critical transformation stress, $\sigma_s^{A \to M}$, increases with temperature when $T > M_s$. The same is valid for $\sigma_s^{M \to A}$ when $T \geq A_s$. Figure 4 shows these critical stresses plotted against temperature. The slopes of the linear regression lines are used to determine the C_M and C_A. The critical stress value at $-53\,°C$ can be included in the interpolation, since it is taken at the M_s of AF30 [8].

The materials show some degree of superelasticity at temperatures above A_s, making it possible to obtain material data needed to perform passive damper simulations based on Brinson's model. In Table 3 an overview of the material data is given.
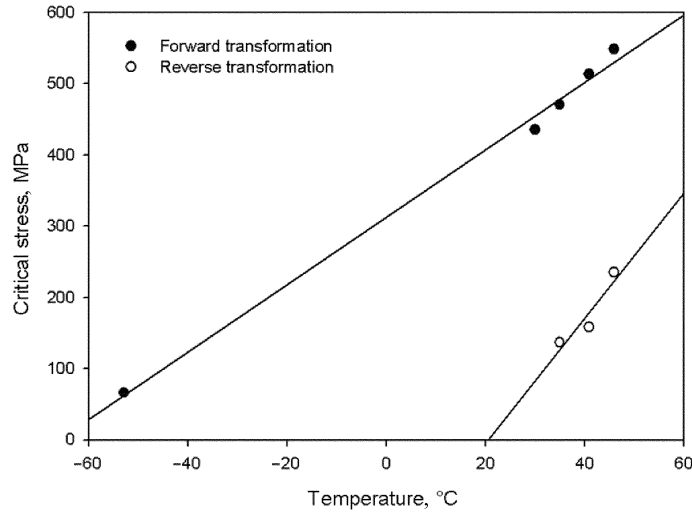
Fig. 4. Critical transformation stresses for forward and reverse transformation as a function of temperature for the AF30 material.

Table 3. Parameters measured from the stress–strain curves for the Brinson model. For explanation of symbols see section 2.2.

Material	D_M, MPa	D_A, MPa	C_M, MPa/°C	C_A, MPa/°C	$\sigma_s^{M'\to M}$, MPa	$\sigma_f^{M'\to M}$, MPa	ε_L
AF5	14 000	62 188	8.0	7.3	72.7	296.9	0.053
AF30	21 784	56 730	4.2	8.8	64.3	394.2	0.047

4. DAMPER DESIGN

The objective of the simulations is to predict the behaviour of seismic dampers with selected composite wires. The dampers are composed of the AF5 and AF30 materials. Each wire has a length of 200 mm and a radius of 1 mm. Springs, dashpots, and spring–dashpot combinations are used to represent super-elasticity (SE), the shape memory effect (SME), and the SE–SME combination, respectively. The SME is used to describe the apparent plastic deformation in the wires. Each damper system consists of three parallel coupled wires. A deformation controlled load-cycle is employed in the simulations as shown schematically in Fig. 5.

Four damper systems were studied. Based on the temperature-dependent behaviour of the wires, i.e. SE and SME, three working temperatures were considered. Since the temperature in the simulations is never below M_s, the wires are all assumed to be 100% austenitic. At temperatures below the A_f of both AF5 and AF30, the wires experience SME and partial SE; when the temperature is above the A_f of AF5 but below the A_f of AF30, both SME and
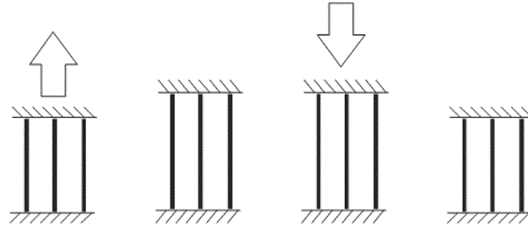
Fig. 5. Deformation controlled load cycle exerted on a seismic damper during simulation.

SE are present; when the temperature is above the A_f of both AF5 and AF30, all wires exhibit SE. Table 4 schematically shows the four damper systems. Three deformation levels were considered for each damper. The deformation length, d_{max}, for each cycle was chosen according to the martensite fraction of the AF5 wires. The martensite control values for simulation are $\xi_{max}^{AF5} = 0.5$, $\xi_{max}^{AF5} = 0.75$, and $\xi_{max}^{AF5} = 1$. They represent the martensite fraction value reached before unloading. Martensite fraction in the AF30 wires differs from the control values due to a shorter transformation length ε_L.

Table 4. Systems and working temperatures considered in the study

Temperature	Combination			
	D 1	D 2	D 3	D 4
0 °C				
25 °C				
45 °C				
	3 x AF5	3 x AF30	2 x AF5 1 x AF30	1 x AF5 2 x AF30

The primary task of a seismic damper is to dissipate energy during seismic activity. The energy dissipation capacities of the four dampers considered in this study are compared in Figs 6 and 7. Figure 6 shows the dissipated energy versus temperature, while Fig. 7 shows the dissipated energy versus ξ_{max}^{AF5} and d_{max}. Figure 6 indicates that the dampers containing homogeneous wire materials experience maximum dissipation when the temperature lies between A_s and A_f. Within this temperature range, however, residual displacement will be present, reducing the re-centring capabilities of the damper. It is therefore desirable to use materials that experience superelasticity when subjected to load in the damper's working temperature. It should be noted that if the temperature is much higher than A_f, the level of dissipated energy decreases noticeably, which is an undesired effect.
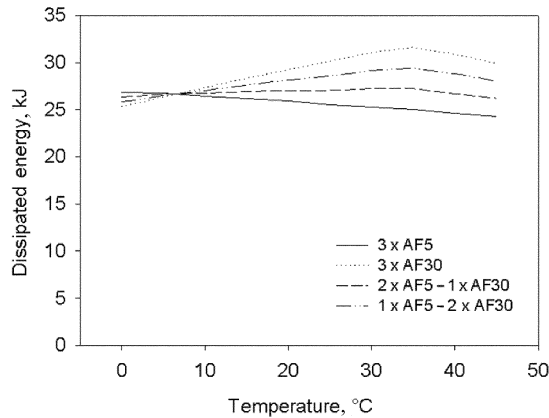

Fig. 6. Comparison of the dissipated energy versus temperature curves.
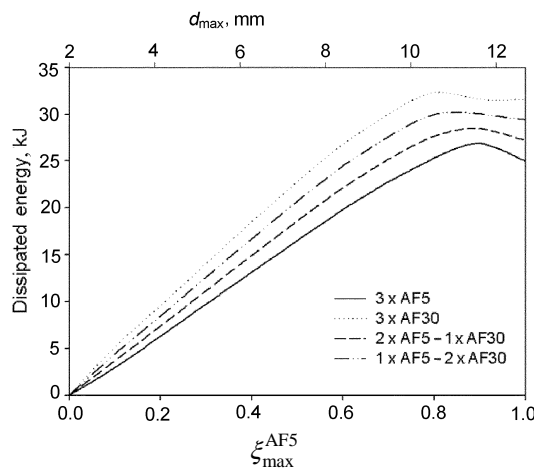

Fig. 7. Dissipated energy versus ξ_{max}^{AF5} for all damper configurations.

Figure 6 shows that a damper containing only the AF30 material exhibits the highest dissipation capacity. But since $A_f = 41\,°C$ for this material, re-centring will not occur at room temperatures. By adding wires of AF5 material, re-centring will occur at all temperatures above $4\,°C$, which is the A_f for the AF5 material. The temperature dependence of the damper is lowest when one AF30 wire is combined with two AF5 wires.

Figure 7 shows how the dissipated energy varies with ξ_{max}^{AF5} and d_{max}. The energy level reaches its maximum in the range $0.8 < \xi_{max}^{AF5} < 0.9$, which indicates that it is not optimal to let the wires be deformed until complete martensite transformation has occurred.

5. CONCLUSIONS

In this work, two commercial NiTi alloys were characterized and their mechanical behaviour in various damper configurations was modelled. The two alloys show only a small temperature region with pseudoelastic behaviour. The damping capacity of the materials is at its maximum just below A_f. Combination of different materials in the same damper configuration results in a broader temperature range with good damping characteristics.

REFERENCES

1. Saadat, S., Salichs, J., Noori, M., Hou, Z., Davoodi, H., Bar-on, I., Suzuki, Y. and Masuda, A. An overview of vibration and seismic application of NiTi shape memory alloy. *Smart Mat. Struct.*, 2002, **11**, 218–229.
2. van der Eijk, C., Zhang, Z. L. and Akselsen, O. M. Seismic dampers based on shape memory alloys: metallurgical background and modeling. In *Proceedings of Third European Conference on Structural Control, 3ECSC, Vienna, Austria, 12–15 July 2004* (Flesch, R. et al., eds). Vienna University of Technology, 2005, M1–5.
3. Song, G., Ma, N. and Li, H.-N. Applications of shape memory alloys in civil structures. *Eng. Struct.*, 2006, **28**, 1266–1274.
4. Janke, L., Czaderski, C., Motavalli, M. and Ruth, J. Applications of shape memory alloys in civil engineering structures – overview, limits and new ideas. *Mat. Struct.*, 2005, **38**, 578–592.
5. Dolce, M. and Cardone, D. Mechanical behaviour of shape memory alloys for seismic applications; 2. Austenite NiTi wires subjected to tension. *Int. J. Mech. Sci.*, 2001, **43**, 2657–2677.
6. Otsuka, K. and Ren, X. Physical metallurgy of Ti-Ni-based shape memory alloys. *Progress Mat. Sci.*, 2005, **50**, 511–678.
7. van der Eijk, C., Olsen, J. S. and Zhang, Z. L. Fitness for purpose evaluation of two NiTi alloys for seismic damping. In *Proceedings of Fourth World Conference on Structural Control and Monitoring (4WCSCM)*, *11–13 July 2006*, *San Diego*, *California*, *U.S.A.* (to appear).
8. Brinson, L. C. One-dimensional constitutive behaviour of shape memory alloys: thermo-mechanical derivation with non-constant material functions and redefined martensite internal variable. *J. Intell. Mat. Systems Struc.*, 1993, **4**, 229–242.
9. Olsen, J. S. *Seismic Dampers with Composite NiTi-Wires – A New Damper System*. M.Sc. thesis, Norwegian University of Science and Technology (NTNU), Trondheim, Norway 2006.

Kahe tööstusliku NiTi sulami pseudoelastse käitumise uurimine: katsed ja modelleerimine

Casper van der Eijk, Jim Stian Olsen ja Zhiliang Z. L. Zhang

On katsetatud tööstuslikke NiTi sulameid seismilise kaitsematerjalina. On määratud kahe erineva NiTi sulami mehaanilised omadused. Üks neist sulamitest on toatemperatuuril täielikult austeniitne, samal ajal kui teise austeniitne faas algab toatemperatuurist kõrgemal temperatuuril, aga martensiitse faasi algus-temperatuur jääb toatemperatuurist allapoole. Neid kaht sulamit iseloomustab pseudoelastne käitumine kitsas temperatuurivahemikus. Modelleerimisel on uuritud, kas kahe erineva materjali kasutamine ühes amortisaatoris võimaldab luua amortisaatorit laia temperatuurivahemiku jaoks ja tagada seejuures head amortiseerivad omadused.